

## 1 **Supplemental Materials**

2 Experimental method:

### 3 **Serum Biochemistry**

4 Blood was collected via cardiac puncture under deep anesthesia. Serum was separated by  
5 centrifugation at  $3,000 \times g$  for 10 minutes at  $4^{\circ}\text{C}$ . Serum creatinine and blood urea nitrogen  
6 (BUN) were measured to assess renal function. Hepatic injury was evaluated by serum alanine  
7 aminotransferase (ALT) and aspartate aminotransferase (AST) activity. All biochemical  
8 parameters were analyzed using commercial colorimetric assay kits according to the  
9 manufacturer's protocols.

### 10 **Histopathological Analysis**

11 Kidney and liver tissues were fixed in 10% neutral buffered formalin for 24 hours, processed,  
12 and embedded in paraffin. Sections ( $4 \mu\text{m}$ ) were stained with hematoxylin and eosin (H&E) for  
13 morphological evaluation. Renal tubular injury was assessed based on tubular necrosis, cast  
14 formation, and brush border loss. Hepatic injury was evaluated by examining hepatocyte  
15 architecture, sinusoidal congestion, and inflammatory infiltration.

16 For lipid accumulation analysis, frozen liver sections ( $8 \mu\text{m}$ ) were prepared using optimal cutting  
17 temperature (OCT) compound. Sections were stained with commercially available Oil Red O  
18 staining kit (Abcam).

### 19 **Quantitative Proteomics**

20 Peptides were analyzed using a Q Exactive HF-X hybrid quadrupole-Orbitrap mass spectrometer  
21 (Thermo Fisher Scientific) coupled to an Easy-nLC 1200 system (Thermo Fisher Scientific).

22 Samples were loaded onto an Acclaim PepMap 100 trap column (75  $\mu\text{m}$   $\times$  2 cm, C18, 3  $\mu\text{m}$ , 100  
23  $\text{\AA}$ ) and separated on an Easy-Spray analytical column (75  $\mu\text{m}$   $\times$  25 cm, C18, 100  $\text{\AA}$ ) at a flow  
24 rate of 300 nL/min. A 120-minute gradient was employed: mobile phase B (0.1% formic acid in  
25 90% acetonitrile) was increased from 2% to 28% over 100 min, then to 40% over 10 min,  
26 followed by a wash at 90% B for 15 min. Mobile phase A consisted of 0.1% formic acid in water.

27 The mass spectrometer was operated with a spray voltage of 2 kV and capillary temperature of  
28 300°C. Full MS scans were acquired at a resolution of 60,000 (AGC target  $3 \times 10^6$ , maximum  
29 injection time 50 ms) over a mass range of 400–1,600 m/z. Data-dependent MS/MS acquisition  
30 selected the top 30 precursor ions with an isolation window of 1.6 m/z, resolution of 15,000  
31 (AGC target  $1 \times 10^4$ , maximum injection time 50 ms), and dynamic exclusion of 25 s.

32 Raw data were processed using MaxQuant (v2.0) with the Andromeda search engine against the  
33 UniProt mouse proteome database. Search parameters included trypsin digestion with up to two  
34 missed cleavages, precursor mass tolerance of 10 ppm, and fragment mass tolerance of 20 ppm.  
35 Variable modifications included methionine oxidation and N-terminal acetylation;  
36 carbamidomethylation of cysteine was set as a fixed modification. Label-free quantification  
37 (LFQ) was enabled with match-between-runs. A false discovery rate (FDR) of 1% was applied at  
38 both peptide and protein levels.

### 39 **Data Analysis**

40 LFQ proteomics data were processed using a custom Snakemake pipeline (v4.5.2).  
41 Contaminants, reverse sequences, and proteins identified only by site were excluded. Proteins  
42 with fewer than two unique peptides were removed. To ensure reliable quantification, proteins  
43 were required to have valid intensity values in at least 70% of samples within each experimental

44 group. Missing values were imputed using the QRILC method with a quantile threshold of 0.01,  
45 appropriate for left-censored proteomics data.

46 Differential protein abundance was assessed using DEqMS (v1.28.0), which extends the limma  
47 framework by incorporating peptide count information to more accurately estimate protein  
48 variance. Statistical significance was determined using an adjusted P-value threshold of 0.05  
49 (Benjamini-Hochberg correction) and an absolute  $\log_2$  fold-change threshold of 1.

50 Pathway enrichment analysis employed a hybrid approach combining over-representation  
51 analysis (ORA) and gene set enrichment analysis (GSEA). ORA was applied to significantly  
52 differentially abundant proteins, while GSEA was performed on all detected proteins ranked by  
53 signed significance score ( $-\log_{10}(\text{P-value}) \times \text{sign}(\log_2\text{FC})$ ). Enrichment was tested against  
54 multiple databases: Gene Ontology (Biological Process, Molecular Function, Cellular  
55 Component), KEGG (Kanehisa et al., 2025; Kanehisa and Goto, 2000), Reactome, MSigDB  
56 Hallmark, and WikiPathways. Semantically similar GO terms were collapsed using the simplify  
57 function (similarity cutoff = 0.7, Wang method) from clusterProfiler (v4.18.4). Pathway activity  
58 was inferred using PROGENy, a footprint-based method that estimates the activity of 14  
59 signaling pathways from protein expression changes using a curated set of downstream response  
60 genes.

## 61 **Western Blot Analysis**

62 Liver tissues were flash-frozen in liquid nitrogen and stored at  $-80^\circ\text{C}$  until protein extraction.  
63 Homogenization was carried out using either T-PER™ Tissue Protein Extraction Reagent  
64 (Thermo Fisher Scientific) in combination with the FastPrep-24™ 5G bead-beating system (MP  
65 Biomedicals), following the manufacturer's protocol, or a sucrose-based buffer (300 mM

66 sucrose, 50 mM Tris·HCl pH 7.4, 1 mM EDTA, 1 mM EGTA, 1 mM Na<sub>3</sub>VO<sub>4</sub>, 50 mM NaF,  
67 1 mM DTT, 1 mM PMSF, 1 µg/mL aprotinin, 4 µg/mL leupeptin, and PhosStop; Roche). Proteins  
68 were separated by SDS-PAGE (standard or 4–15% Criterion TGX Stain-Free gels; Bio-Rad) and  
69 transferred to PVDF membranes. Membranes were blocked with 5% nonfat dry milk in TBS-T,  
70 incubated overnight at 4 °C with primary antibodies, and subsequently with secondary antibodies  
71 for 1 h at room temperature. Detection was performed using Western Lightning Plus-ECL  
72 (PerkinElmer) and imaged with the ChemiDoc Imaging System (Bio-Rad). See Supplementary  
73 Table S3 for complete antibody information.

#### 74 **Immunohistochemistry**

75 Paraffin-embedded liver sections (4 µm) were deparaffinized and rehydrated through graded  
76 alcohols. Antigen retrieval was performed using citrate buffer (pH 6.0) in a pressure cooker for  
77 15 minutes. Endogenous peroxidase activity was quenched with 3% H<sub>2</sub>O<sub>2</sub> for 10 minutes.  
78 Sections were blocked with 5% normal serum for 1 hour, then incubated overnight at 4°C with  
79 primary antibodies against CD68 (1:200) or F4/80 (1:200). Detection was performed using a  
80 polymer-based HRP detection system with DAB chromogen. Sections were counterstained with  
81 hematoxylin and mounted. Positive cells were quantified from 5 random high-power fields per  
82 section using ImageJ.

#### 83 **Quantitative Reverse-Transcription PCR**

84 A small piece of freshly harvested liver tissue was immediately kept in RNAlater solution  
85 (Invitrogen, USA) according to the manufacture's protocol. Total RNA was isolated using  
86 TRIzol™ Reagent (Invitrogen, USA) according to the manufacturer's instructions and quantified  
87 by NanoDrop One system (Thermo Fisher Scientific, USA). Then, the RNA was reverse

88 transcribed with iScript Reverse Transcription Supermix (Bio-Rad). qPCR was performed on a  
89 CFX96 real-time system (Bio-Rad). The primers used in this study were listed in Supplementary  
90 Table S4.

### 91 **XBPI Splicing Assay**

92 Activation of the IRE1 $\alpha$  branch of the unfolded protein response was assessed by quantifying  
93 spliced Xbp1 (Xbp1s) mRNA levels. Under ER stress, activated IRE1 $\alpha$  excises a 26-nucleotide  
94 intron from Xbp1 mRNA, generating the transcriptionally active Xbp1s isoform. To specifically  
95 detect this spliced variant, qPCR was performed using primers designed to span the splice  
96 junction ( Forward: 5'-CTGAGTCCGAATCAGGTGCAG-3'; Reverse: 5'-  
97 GGTCCATGGGAAGATGTTCTGG-3'), which selectively amplify Xbp1s but not unspliced  
98 Xbp1u.

99

### 100 **Supplementary Methods: Clinical Cohort Analyses**

#### 101 **Cohort Derivation: MIMIC-IV**

102 The MIMIC-IV (version 3.1) database contained 94,458 ICU admissions. Patients were excluded  
103 sequentially as follows: ICU length of stay shorter than 24 hours (n = 18,786); pre-existing liver  
104 disease identified by ICD-9 code 571.x or ICD-10 codes K70 through K77 (n = 11,584); prior  
105 liver transplantation (n = 202); chronic kidney disease stage 3 or higher, defined by diagnosis  
106 codes or estimated glomerular filtration rate below 60 mL/min/1.73 m<sup>2</sup> calculated using the  
107 CKD-EPI 2021 equation (n = 13,577 by diagnosis codes; n = 4,872 by eGFR); missing baseline  
108 serum creatinine within seven days of ICU admission (n = 830); missing baseline alanine  
109 aminotransferase or aspartate aminotransferase (n = 28,346); and baseline ALT or AST

110 exceeding twice the upper limit of normal (>80 U/L; n = 3,557). After all exclusions, 12,704  
111 patients remained (3,803 with AKI and 8,901 without AKI). A CONSORT-style flow diagram is  
112 presented in Figure 7A.

113 AKI was classified using the Kidney Disease: Improving Global Outcomes (KDIGO) serum  
114 creatinine criteria. Baseline creatinine was defined as the lowest value recorded within the first  
115 seven days of ICU admission. Stage 1 required a rise of 0.3 mg/dL or more within 48 hours, or a  
116 1.5-fold increase above baseline within seven days. Thresholds for Stages 2 and 3 were 2.0-fold  
117 and 3.0-fold increases above baseline, respectively; Stage 3 was also assigned when creatinine  
118 exceeded 4.0 mg/dL or renal replacement therapy was initiated. Urine output criteria were not  
119 used for primary staging.

#### 120 **Propensity Score Matching and Covariate Balance: MIMIC-IV**

121 Propensity scores were estimated using logistic regression with the following covariates: age,  
122 sex, non-renal Sequential Organ Failure Assessment (SOFA) score, Sepsis-3 status, diabetes,  
123 vasopressor use, and admission category (emergency, surgical, elective, or other). Matching was  
124 performed at a 1:1 ratio using nearest-neighbor matching without replacement, with a caliper  
125 width of 0.2 standard deviations of the logit-transformed propensity score (caliper = 0.1399). Of  
126 3,803 eligible AKI patients, 3,498 (92.0%) were successfully matched to 3,498 controls, yielding  
127 a final analytic cohort of 6,996 patients. The remaining 305 AKI patients fell outside the caliper  
128 and were excluded.

129 Covariate balance was assessed using standardized mean differences (SMD), with a threshold of  
130 less than 0.1 indicating adequate balance. All nine matching covariates achieved excellent  
131 balance after matching (Table S5). The maximum SMD decreased from 0.593 (non-renal SOFA

132 score) before matching to 0.037 (age) after matching. Individual covariate SMDs after matching  
133 were as follows: age, 0.037; sex, 0.009; non-renal SOFA score, 0.010; sepsis, 0.016; diabetes,  
134 0.024; vasopressor use, 0.013; emergency admission, 0.034; other admission category, 0.018;  
135 and surgical admission, 0.016. ICU length of stay, hospital mortality, statin use, acetaminophen  
136 exposure, and mechanical ventilation were not included in the propensity model because they  
137 represent post-admission exposures or outcomes that may lie on the causal pathway between  
138 AKI and hepatic dysfunction. Baseline demographics of the matched cohort are reported in Table  
139 3 of the main manuscript.

140 The matched AKI cohort comprised 2,196 patients with KDIGO Stage 1 (62.8%), 866 with Stage  
141 2 (24.8%), and 436 with Stage 3 (12.5%). Both groups were comparable in age (63.1 versus 63.7  
142 years; SMD = 0.037), sex distribution (55.3% versus 54.8% male; SMD = 0.009), non-renal  
143 SOFA score (median 4 in both groups; SMD = 0.010), sepsis prevalence (47.4% versus 48.2%;  
144 SMD = 0.016), diabetes (28.6% versus 27.6%; SMD = 0.024), and vasopressor use (42.7%  
145 versus 42.1%; SMD = 0.013).

#### 146 **Outcome Ascertainment: MIMIC-IV**

147 Peak values for ALT, AST, total bilirubin, and alkaline phosphatase were extracted within 72  
148 hours of AKI onset for AKI patients (or the matched reference time for controls). Albumin nadir  
149 was determined over the same window. Clinically significant liver injury was defined as peak  
150 ALT exceeding twice the upper limit of normal (>80 U/L).

151 Between-group comparisons used the Mann-Whitney U test. Severity-dependent relationships  
152 across KDIGO stages were evaluated using Kruskal-Wallis and Jonckheere-Terpstra trend tests.

153 Temporal trajectories of liver markers were modeled with linear mixed-effects models

154 incorporating log-transformed values, a time-by-group interaction term, and a random intercept  
155 per patient. Multivariable logistic regression estimated the adjusted odds of liver injury,  
156 controlling for age, sex, non-renal SOFA score, sepsis status, vasopressor use, diabetes, statin  
157 use, acetaminophen exposure, and mechanical ventilation.

#### 158 **Sensitivity Analyses: MIMIC-IV**

159 Four pre-specified sensitivity analyses were conducted: (1) stricter baseline exclusion requiring  
160 ALT and AST both below the upper limit of normal (40 U/L); (2) analysis of the full unmatched  
161 cohort (n = 12,704) with multivariable adjustment; (3) liver injury defined by AST rather than  
162 ALT (AST >80 U/L); and (4) exclusion of patients who received potentially hepatotoxic  
163 antibiotics during the ICU stay.

#### 164 **Cohort Derivation: eICU-CRD**

165 The eICU Collaborative Research Database (eICU-CRD, version 2.0) contained 200,859 ICU  
166 admissions from 208 hospitals across the United States during 2014 and 2015. Patients were  
167 excluded sequentially: age younger than 18 years (n = 530); pre-existing end-stage renal disease  
168 or chronic dialysis, identified from diagnosis codes and past medical history fields (n = 8,216);  
169 ICU length of stay shorter than 24 hours (n = 65,539); pre-existing liver cirrhosis (n = 4,101);  
170 and absence of serum creatinine data (n = 5,347). The final analytic cohort comprised 117,126  
171 ICU stays, of which 24,905 (21.3%) met KDIGO creatinine criteria for AKI: 14,920 Stage 1  
172 (12.7%), 1,961 Stage 2 (1.7%), and 8,024 Stage 3 (6.9%).

173 Baseline creatinine in the eICU-CRD analysis was defined as the first serum creatinine measured  
174 within 24 hours of ICU admission, with fallback to the lowest value within 48 hours if no  
175 measurement was available in the first 24 hours. AKI staging followed the same KDIGO

176 creatinine thresholds described for MIMIC-IV. Renal replacement therapy initiation was  
177 identified from the treatment table and APACHE assessment variables to capture additional  
178 Stage 3 patients.

#### 179 **Lipid Measurements: eICU-CRD**

180 Serum lipid measurements (triglycerides, total cholesterol, HDL cholesterol, and LDL  
181 cholesterol) were extracted from the laboratory table using verified labName strings.  
182 Measurement timestamps were derived from the labResultOffset variable, expressed as minutes  
183 from ICU admission. Pre-admission measurements (negative offset values) were excluded from  
184 the primary analysis, yielding 80,690 post-admission lipid measurements. After outlier removal  
185 (triglycerides below 10 mg/dL or above 10,000 mg/dL; total cholesterol below 20 mg/dL or  
186 above 1,000 mg/dL; LDL below 1 mg/dL or above 500 mg/dL; 17 values excluded total),  
187 102,725 clean lipid measurements from 28,519 patients were available for analysis. Among  
188 these, 22,727 patients had at least one triglyceride measurement (5,956 AKI; 16,771 non-AKI),  
189 16,205 had total cholesterol, 16,226 had HDL, and 12,017 had LDL data.

#### 190 **Statistical Analysis: eICU-CRD**

191 Primary comparisons of lipid levels between AKI and non-AKI groups used Mann-Whitney U  
192 tests, given non-normal distributions. Effect sizes were reported as rank-biserial correlation  
193 coefficients and Cohen's d. Stratified analyses by KDIGO stage used Kruskal-Wallis tests with  
194 post-hoc Bonferroni-corrected pairwise comparisons. Multivariable linear regression of log-  
195 transformed lipid values was performed with adjustment for age, sex, APACHE IV score, body  
196 mass index (BMI), and diabetes status. Subgroup analyses examined the consistency of lipid  
197 associations across sepsis status, surgical versus medical admission, sex, and diabetes.

198 Temporal analysis used measurements binned into six time windows (0-24h, 24-48h, 48-72h, 72-  
199 96h, 4-7 days, and >7 days). For patients with two or more triglyceride measurements (n =  
200 4,654), a linear mixed-effects model was fitted using restricted maximum likelihood (REML)  
201 estimation. Log-transformed triglycerides served as the outcome. Fixed effects included time  
202 (days), AKI status, and their interaction, with adjustment for age, sex, APACHE IV score, BMI,  
203 and diabetes; a random intercept was specified for each patient. A secondary AKI definition  
204 based on diagnosis codes was used for sensitivity analysis, confirming concordant results  
205 (median TG 132 versus 111 mg/dL;  $p = 8.3 \times 10^{-48}$ ).

## 206 **Cross-Database Comparison**

207 Triglyceride levels were compared between the eICU-CRD primary analysis (n = 22,727) and an  
208 exploratory subset from MIMIC-IV with available triglyceride data (AKI n = 175; control n =  
209 55). Both databases showed significantly elevated triglycerides in the AKI group (eICU-CRD:  
210 124 versus 111 mg/dL,  $p = 4.9 \times 10^{-40}$ ; MIMIC-IV: 269 versus 188 mg/dL,  $p < 0.001$ ). Absolute  
211 triglyceride values differed between databases, likely reflecting differences in measurement  
212 timing (median first triglyceride measurement at 16 to 36 hours post-admission in eICU-CRD  
213 versus peri-AKI onset sampling in MIMIC-IV), population characteristics (multi-center versus  
214 single-center), and the smaller MIMIC-IV lipid subset. The direction and statistical significance  
215 of the AKI-associated triglyceride elevation were concordant across both databases.

## 216 **Software**

217 All clinical analyses were performed in Python 3.9.6 using the following packages: pandas 2.3.3  
218 for data manipulation, scipy 1.13.1 for non-parametric statistical tests, statsmodels 0.14.6 for  
219 regression modeling and mixed-effects models, tableone 0.9.6 for demographic table generation,

220 matplotlib 3.9.4 and seaborn 0.13.2 for visualization, and google-cloud-bigquery 3.40.1 for  
221 eICU-CRD database access. Propensity score estimation and matching for the MIMIC-IV  
222 analysis used statsmodels logistic regression with nearest-neighbor matching implemented via  
223 custom scripts. A two-sided p-value below 0.05 was considered statistically significant  
224 throughout.

225

226

## 227 **Supplementary Figure Legends**

### 228 **Supplementary Figure 1. AKI Validation and Inflammatory Profiling**

229 (A) Plasma creatinine levels in Sham and AKI mice at 24 hours post-surgery, confirming  
230 successful induction of kidney injury. Data are presented as mean  $\pm$  SD. \* $p < 0.05$  by unpaired  
231 Student's t-test. (B) Cytokine array analysis of liver tissue samples from Sham and AKI mice.  
232 Representative array membranes showing relative abundance of inflammatory cytokines and  
233 chemokines. Overall cytokine levels are reduced in AKI compared to Sham, consistent with the  
234 paradoxical suppression of inflammatory output described in the main text. (C) Densitometric  
235 quantification of selected pro-inflammatory cytokines (TNF- $\alpha$ , IL-1 $\beta$ , IL-6) from the cytokine  
236 array membranes shown in (B). Values are normalized to Sham controls and expressed as relative  
237 blot density. Despite TLR4/MyD88 activation in AKI livers, circulating levels of these canonical  
238 inflammatory mediators trended lower in AKI animals, though differences did not reach  
239 statistical significance (ns, not significant). Data are presented as mean  $\pm$  SD; unpaired Student's  
240 t-test.

241 **Supplementary Figure 2. Transcript-Level Validation of Key Signaling and Metabolic**  
242 **Genes**

243 (A) Quantitative RT-PCR analysis of TLR4 co-receptors. CD14 transcript levels are significantly  
244 upregulated in AKI livers, while MD-2 shows no significant change. (B) Quantitative RT-PCR  
245 analysis of macrophage markers. F4/80 expression is significantly reduced, CD68 is significantly  
246 increased, and CD163 is significantly upregulated in AKI livers. (C) Quantitative RT-PCR  
247 analysis of fatty acid handling genes. Fabp1 expression is significantly reduced, while Acox1  
248 shows a compensatory increase in AKI livers. Expression normalized to GAPDH and presented  
249 relative to Sham controls. Data are mean  $\pm$  SEM; n=5 per group. \*p < 0.05 by unpaired two-  
250 tailed Student's t-test.

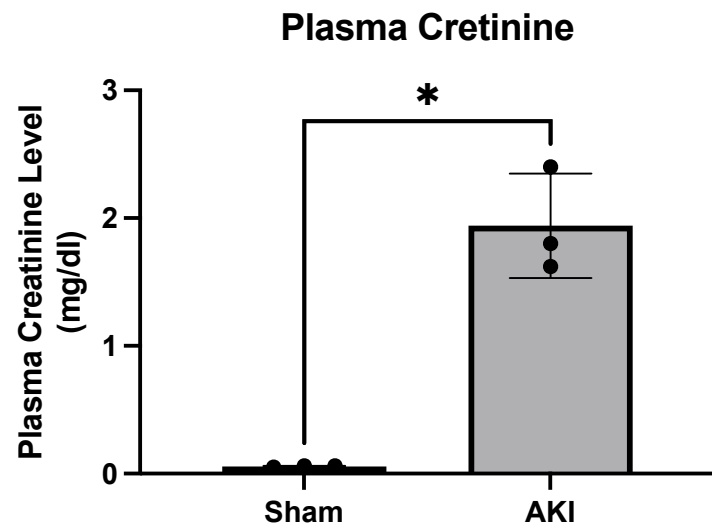
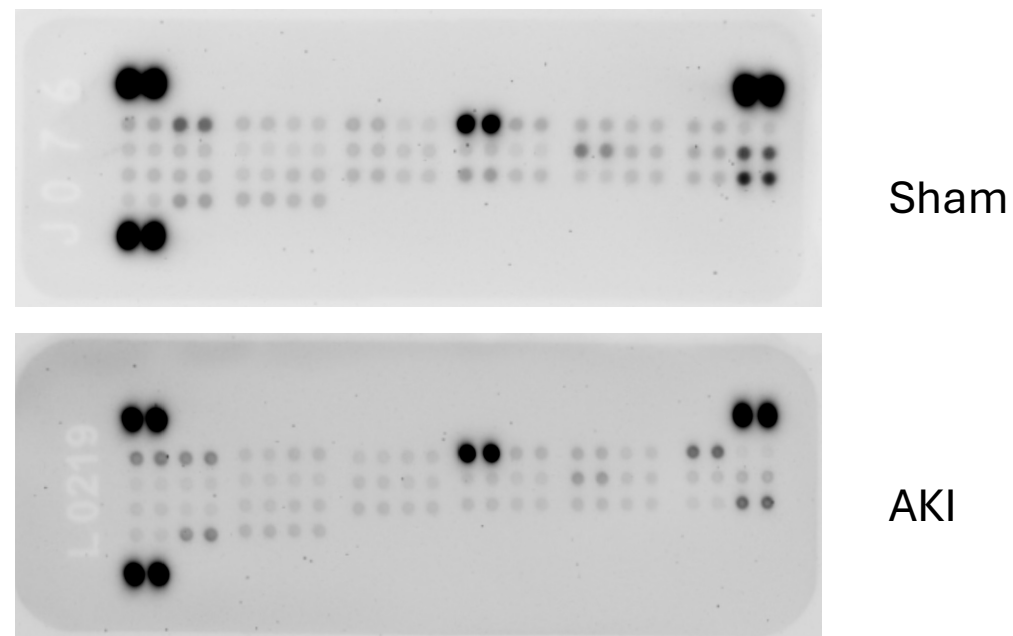
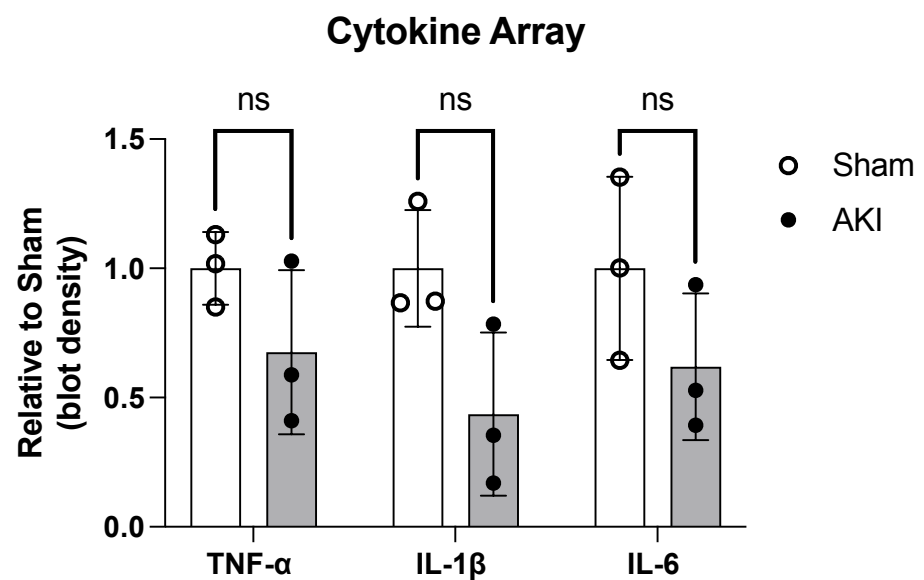
251 **Supplementary Figure 3. Comprehensive Pathway Enrichment Analysis**

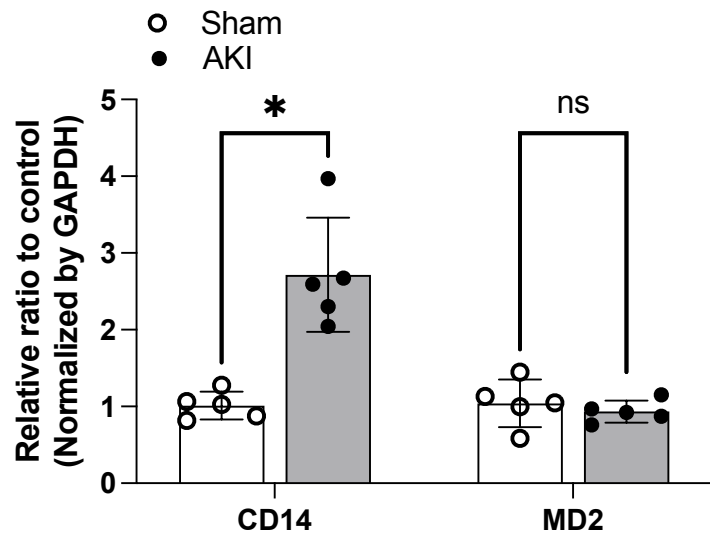
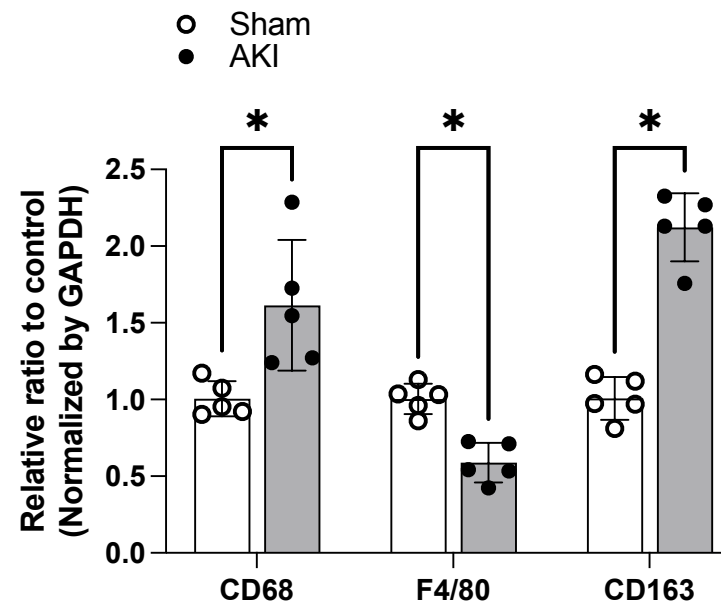
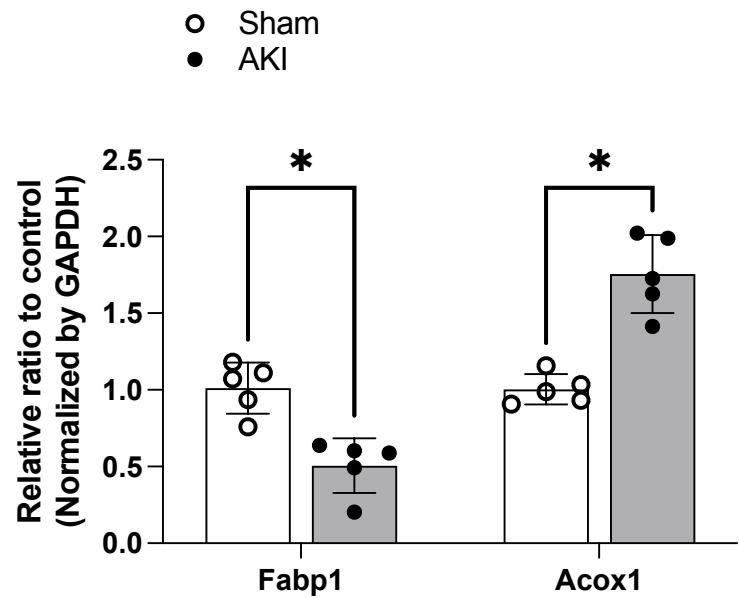
252 (A) MSigDB Hallmark gene set enrichment analysis (GSEA) showing enriched pathways in AKI  
253 livers. Dot size represents gene count; color indicates adjusted p-value. (B) KEGG pathway  
254 enrichment analysis showing additional dysregulated pathways in AKI livers, including  
255 xenobiotic metabolism and steroid hormone biosynthesis. Dot size represents gene count; color  
256 indicates adjusted p-value. Pathway annotations in panel B were obtained from the KEGG  
257 database (Kanehisa et al., 2025; Kanehisa and Goto, 2000).

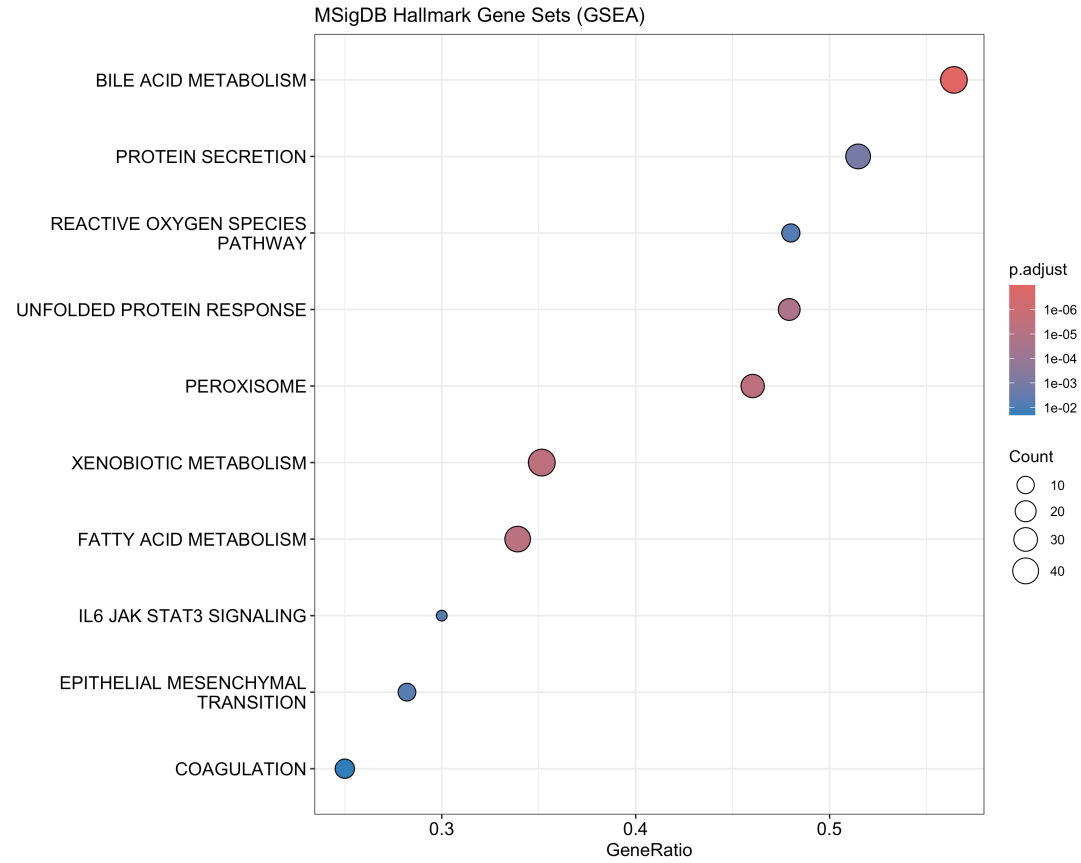
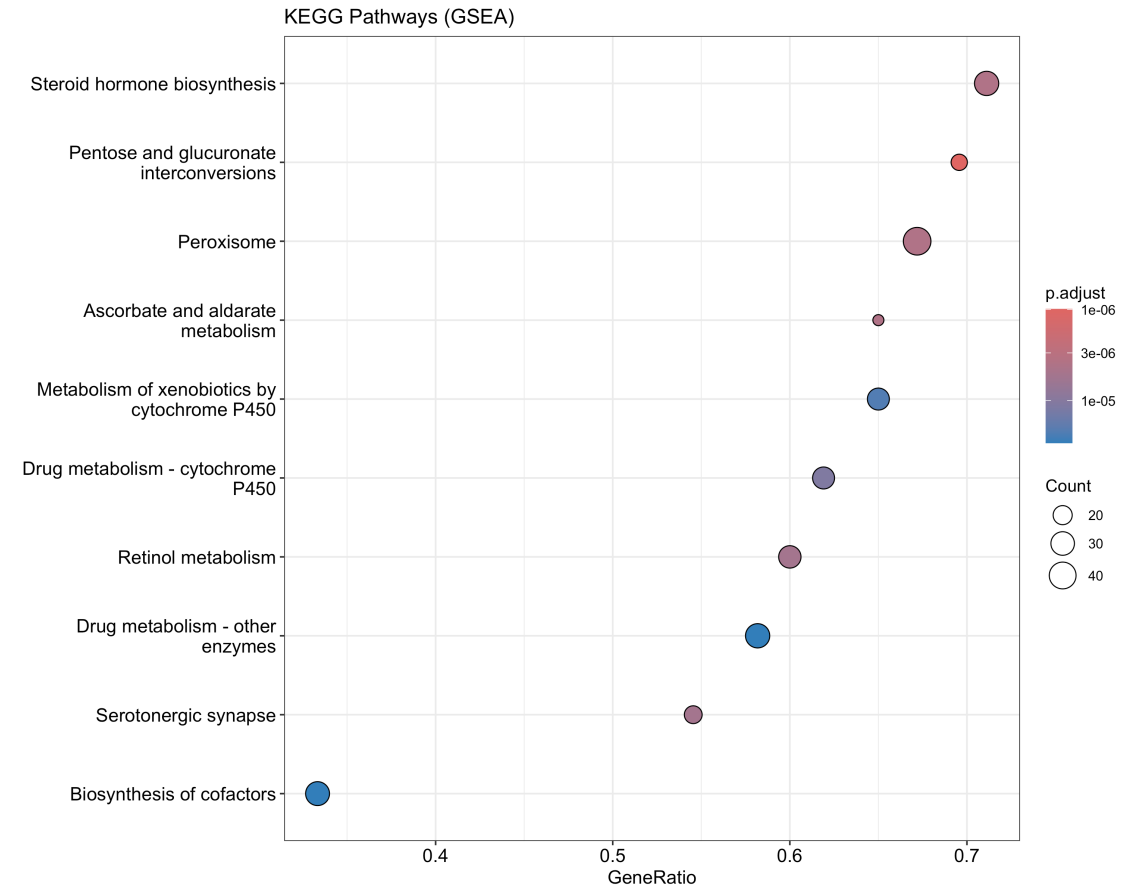
258 **Supplementary Figure 4. Cross-Database Comparison of Serum Triglyceride Levels in**  
259 **Acute Kidney Injury**

260 (A) Forest plot showing percent change in serum triglycerides associated with AKI across two  
261 independent ICU databases (eICU-CRD, multi-center, 208 hospitals; MIMIC-IV, single-center).  
262 eICU-CRD analyses include unadjusted and covariate-adjusted estimates (adjusted for age, sex,

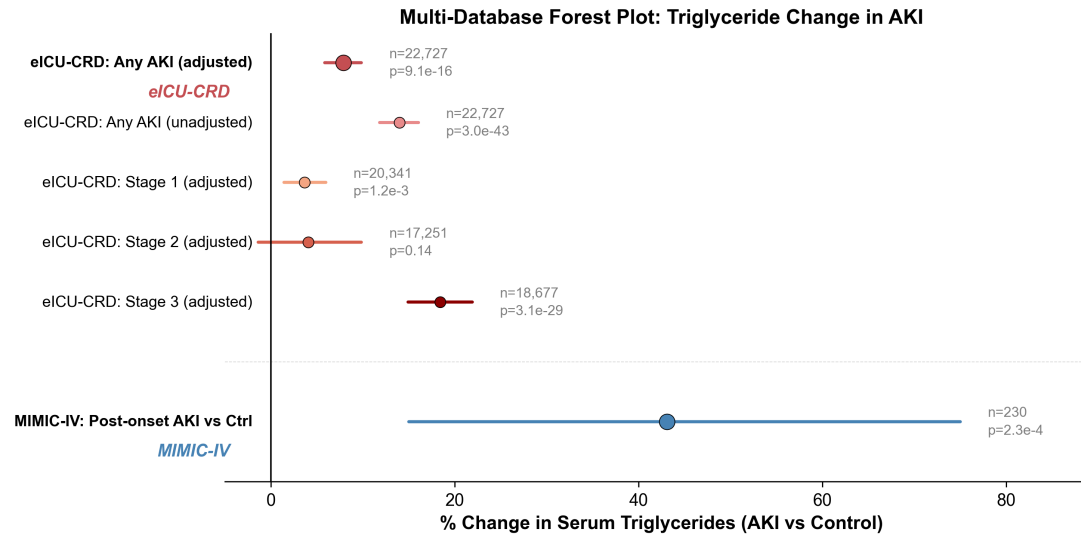
263 APACHE IV score, BMI, and diabetes) along with KDIGO stage-specific effects. Error bars  
264 represent 95% confidence intervals. (B) Median triglyceride levels with interquartile range in  
265 AKI versus non-AKI groups in each database. Solid bars indicate eICU-CRD; hatched bars  
266 indicate MIMIC-IV. \*\*\* $p < 0.001$ . (C) Lipid dissociation pattern in eICU-CRD: percent change  
267 in four serum lipid markers (triglycerides, total cholesterol, HDL, LDL) in AKI compared with  
268 non-AKI patients. Triglycerides were elevated (+11.7%) while total cholesterol, HDL, and LDL  
269 were all reduced (range: -10.3% to -15.4%).

**A.****B.****C.**

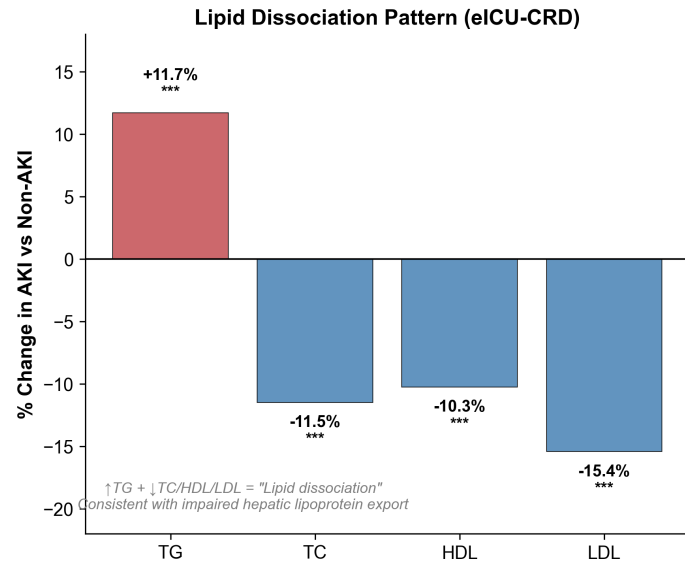
**A.****B.****C.**

**A.****B.**

A.



B.



C.

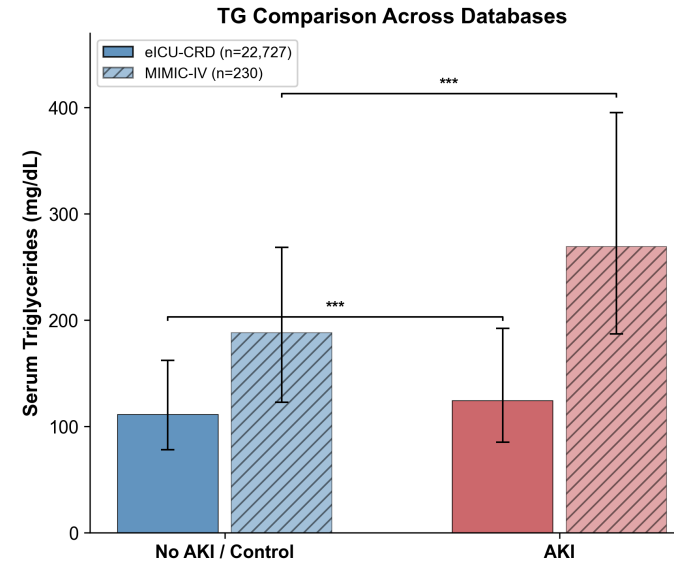


**Table S1. Complete list of differentially expressed proteins in liver tissue 24 hours post-AKI**

Protein ID	Gene Symbol	Protein Name	log2FC (AKI/Sham)	P-value	Adjusted P-value (FDR)	Mean Intensity Sham	Mean Intensity AKI	Regulation
Q3TF08	<i>Rbp4</i>	Retinol-binding protein 4	-3.47	8.58E-11	3.06E-07	24.73	21.26	DOWN
O55239	<i>Nnmt</i>	Nicotinamide N-methyltransferase	2.72	1.39E-09	2.22E-06	23.66	26.38	UP
Q91XL1	<i>Lrg1</i>	Lrg1 protein	3.99	1.87E-09	2.22E-06	21.43	25.42	UP
E9PV24	<i>Fga</i>	Fibrinogen alpha chain	2.54	3.32E-09	2.96E-06	25.52	28.06	UP
Q3UBS3	<i>Hp</i>	Haptoglobin	2.45	7.70E-09	5.50E-06	25.81	28.25	UP
Q505A3	<i>B3galt1</i>	Hexosyltransferase	2.73	1.12E-08	5.78E-06	19.55	22.28	UP
I3PQW8	<i>Tifa</i>	TRAF-interacting protein with FHA domain-containing protein A	4.92	1.13E-08	5.78E-06	18.11	23.03	UP
Q6NWW9	<i>Fndc3b</i>	Fibronectin type III domain-containing protein 3B	4.26	1.61E-08	6.92E-06	19.01	23.27	UP
A0A1B0GQV5	<i>Saa2</i>	Serum amyloid A protein	10.91	1.75E-08	6.92E-06	17.20	28.10	UP
P01027	<i>C3</i>	Complement C3	1.13	2.00E-08	7.12E-06	26.13	27.27	UP
E9PVD2	<i>Itih4</i>	Itih4 protein	2.48	3.66E-08	1.16E-05	24.07	26.55	UP
A7E1Z5	<i>Slc4a4</i>	Anion exchange protein	1.46	5.95E-08	1.63E-05	22.19	23.65	UP

Protein ID	Gene Symbol	Protein Name	log2FC (AKI/Sham)	P-value	Adjusted P-value (FDR)	Mean Intensity Sham	Mean Intensity AKI	Regulation
P11672	<i>Lcn2</i>	Neutrophil gelatinase-associated lipocalin	7.76	6.67E-08	1.70E-05	19.12	26.89	UP
Q8QZR1	<i>Tat</i>	Tyrosine aminotransferase	2.40	8.76E-08	1.92E-05	24.05	26.45	UP
Q61838	<i>A2m</i>	Pregnancy zone protein	1.28	9.66E-08	1.92E-05	25.73	27.01	UP
Q3UER8	<i>Fgg</i>	Fibrinogen gamma chain	2.17	9.68E-08	1.92E-05	26.14	28.30	UP
Q6S9I0	<i>Kn2</i>	Kn2 protein	3.41	1.69E-07	3.14E-05	18.90	22.31	UP
Q3TGR2	<i>Fgb</i>	Fibrinogen beta chain	2.37	1.94E-07	3.14E-05	25.42	27.78	UP
Q4JFI8	<i>Apcs</i>	Pentraxin family member	5.36	2.86E-07	3.68E-05	19.43	24.79	UP
Q3UWC2	<i>Saa1</i>	Serum amyloid A protein	7.67	3.07E-07	3.78E-05	20.47	28.13	UP
Q07456	<i>Ambp</i>	Protein AMBP	1.07	3.23E-07	3.79E-05	23.46	24.54	UP
Q03734	<i>Serpina3m</i>	Serine protease inhibitor A3M	4.26	3.29E-07	3.79E-05	21.34	25.60	UP
Q9CR29	<i>Ccdc43</i>	Coiled-coil domain-containing protein 43	2.95	3.95E-07	4.14E-05	19.15	22.10	UP
Q91X72	<i>Hpx</i>	Hemopexin	1.73	6.33E-07	6.09E-05	24.89	26.62	UP
Q545K5	<i>Rbm3</i>	RNA-binding protein 3	2.29	6.49E-07	6.09E-05	22.91	25.20	UP
P58710	<i>Gulo</i>	L-gulonolactone oxidase	-1.07	7.22E-07	6.48E-05	28.67	27.60	DOWN
A0A0R4J0N7	<i>Cyp8b1</i>	Cyp8b1 protein	-1.05	7.26E-07	6.48E-05	25.79	24.74	DOWN

Protein ID	Gene Symbol	Protein Name	log2FC (AKI/Sham)	P-value	Adjusted P-value (FDR)	Mean Intensity Sham	Mean Intensity AKI	Regulation
Q3UEK1	<i>Mbl2</i>	Mannose-binding protein C	-1.48	7.60E-07	6.61E-05	24.37	22.88	DOWN
P23953	<i>Ces1c</i>	Carboxylesterase 1C	-1.25	9.60E-07	7.61E-05	24.67	23.42	DOWN
F2WWK6	<i>Fads2</i>	Acyl-CoA 6-desaturase	-1.21	1.35E-06	1.02E-04	24.64	23.43	DOWN
P21981	<i>Tgm2</i>	Protein-glutamine gamma-glutamyltransferase 2	1.03	1.79E-06	1.31E-04	26.15	27.18	UP
Q91X83	<i>Mat1a</i>	S-adenosylmethionine synthase isoform type-1	1.46	1.90E-06	1.36E-04	29.37	30.83	UP
Q9CQW9	<i>Ifitm3</i>	Interferon-induced transmembrane protein 3	1.30	1.99E-06	1.36E-04	24.37	25.67	UP
Q61704	<i>Itih3</i>	Inter-alpha-trypsin inhibitor heavy chain H3	4.68	2.05E-06	1.38E-04	18.85	23.53	UP
Q923B6	<i>Steap4</i>	Metalloreductase STEAP4	2.73	2.48E-06	1.64E-04	25.67	28.40	UP
Q3U8S0	<i>Ap3s1</i>	Ap3s1 protein	3.74	3.34E-06	2.13E-04	19.08	22.82	UP
Q566J8	<i>Adck4</i>	Atypical kinase COQ8B, mitochondrial	4.34	3.63E-06	2.23E-04	18.80	23.14	UP
Q99J93	<i>Ifitm2</i>	Interferon-induced transmembrane protein 2	2.07	3.98E-06	2.41E-04	22.89	24.97	UP
Q3UKN6	<i>Nucb2</i>	Nucb2 protein	3.61	6.69E-06	3.85E-04	20.15	23.76	UP
Q4FJR9	<i>Isg15</i>	Ubiquitin-like protein ISG15	-3.12	7.43E-06	4.21E-04	22.63	19.51	DOWN
Q3U5H8	<i>Hmox1</i>	Heme oxygenase 1	4.52	1.20E-05	6.17E-04	19.34	23.86	UP

Protein ID	Gene Symbol	Protein Name	log2FC (AKI/Sham)	P-value	Adjusted P-value (FDR)	Mean Intensity Sham	Mean Intensity AKI	Regulation
Q8VCC1	<i>Hpgd</i>	15-hydroxyprostaglandin dehydrogenase [NAD(+)]	-3.29	1.69E-05	7.66E-04	23.73	20.43	DOWN
Q9QXT7	<i>C6</i>	C6 protein	-2.58	1.84E-05	8.01E-04	24.13	21.55	DOWN
Q3KQQ2	<i>Mup3</i>	Mup3 protein	-1.01	1.94E-05	8.15E-04	27.46	26.45	DOWN
A0A0R4J0E1	<i>Fgl1</i>	Fibrinogen-like protein 1	5.17	2.23E-05	9.00E-04	19.36	24.54	UP
A2A5E1	<i>Dnajc7</i>	DnaJ homolog subfamily C member 7	3.68	2.44E-05	9.24E-04	19.06	22.73	UP
E0CYH9	<i>Nos1ap</i>	Nos1ap protein	2.99	2.45E-05	9.24E-04	18.90	21.89	UP
P41233	<i>Abca1</i>	Phospholipid-transporting ATPase ABCA1	2.55	3.47E-05	1.17E-03	21.22	23.78	UP
Q5FW60	<i>Mup20</i>	Major urinary protein 20	-1.41	3.61E-05	1.20E-03	28.91	27.50	DOWN
E9QAH1	<i>Golgb1</i>	Golgb1 protein	1.81	4.13E-05	1.33E-03	21.29	23.10	UP
Q80VJ2	<i>Sra1</i>	Steroid receptor RNA activator 1	1.00	5.67E-05	1.67E-03	22.33	23.33	UP
P07309	<i>Ttr</i>	Transthyretin	-1.05	5.96E-05	1.73E-03	26.61	25.56	DOWN
Q6P200	<i>Cyp17a1</i>	Steroid 17-alpha-hydroxylase/17,20 lyase	2.40	8.12E-05	2.16E-03	19.61	22.01	UP
O70570	<i>Pigr</i>	Polymeric immunoglobulin receptor	-2.02	9.14E-05	2.32E-03	24.35	22.33	DOWN
Q80XK1	<i>Cyp2a5</i>	Cytochrome P450	-1.39	1.09E-04	2.60E-03	26.37	24.98	DOWN

Protein ID	Gene Symbol	Protein Name	log2FC (AKI/Sham)	P-value	Adjusted P-value (FDR)	Mean Intensity Sham	Mean Intensity AKI	Regulation
Q9BCZ4	<i>Vimp</i>	Selenoprotein S	3.51	1.13E-04	2.65E-03	19.89	23.39	UP
Q64726	<i>Azgp1</i>	Zinc-alpha-2-glycoprotein	-1.52	1.28E-04	2.89E-03	23.42	21.90	DOWN
Q60590	<i>Orm1</i>	Alpha-1-acid glycoprotein 1	2.44	1.33E-04	2.95E-03	23.27	25.71	UP
A1L3S6	<i>Cyp7a1</i>	Cholesterol 7-alpha-monooxygenase	-2.70	1.45E-04	3.11E-03	24.05	21.35	DOWN
G3X8T9	<i>Serpina3n</i>	Serpina3n protein	5.06	1.52E-04	3.21E-03	20.54	25.61	UP
F2Z3U3	<i>Raph1</i>	Raph1 protein	1.32	1.58E-04	3.29E-03	22.25	23.57	UP
A0A077S2U6	<i>Lyz2</i>	lysozyme	3.78	1.87E-04	3.66E-03	19.79	23.56	UP
Q9D566	<i>Sult1e1</i>	Sulfotransferase	4.19	2.13E-04	4.02E-03	18.70	22.90	UP
P02802	<i>Mt1</i>	Metallothionein-1	6.01	2.62E-04	4.58E-03	23.42	29.42	UP
Q3TDW9	<i>Ralbp1</i>	Ralbp1 protein	-1.51	2.65E-04	4.58E-03	20.30	18.79	DOWN
A0A0N4SVU8	<i>Tmem176a</i>	Tmem176a protein	2.58	2.92E-04	4.90E-03	19.22	21.79	UP
Q3U711	<i>Plin2</i>	Perilipin	2.00	3.54E-04	5.59E-03	24.03	26.02	UP
P60824	<i>Cirbp</i>	Cold-inducible RNA-binding protein	2.69	3.99E-04	6.10E-03	19.18	21.87	UP
A0A0A6YW87	<i>Cnih4</i>	Cnih4 protein	-3.59	4.14E-04	6.26E-03	22.56	18.96	DOWN
Q4FK16	<i>Plscr1</i>	Phospholipid scramblase	1.04	4.30E-04	6.44E-03	22.69	23.73	UP

<b>Protein ID</b>	<b>Gene Symbol</b>	<b>Protein Name</b>	<b>log2FC (AKI/Sham)</b>	<b>P-value</b>	<b>Adjusted P-value (FDR)</b>	<b>Mean Intensity Sham</b>	<b>Mean Intensity AKI</b>	<b>Regulation</b>
Q75N73	<i>Slc39a14</i>	Metal cation symporter ZIP14	1.59	4.35E-04	6.48E-03	23.62	25.22	UP
Q8VC77	<i>Akr1c20</i>	Akr1c20 protein	-1.23	4.84E-04	6.99E-03	24.05	22.82	DOWN
A2CEK7	<i>Mup14</i>	Mup14 protein	-1.22	6.67E-04	8.94E-03	31.68	30.46	DOWN
A2AKN8	<i>Mup8</i>	Mup8 protein	-1.32	8.02E-04	1.02E-02	28.34	27.02	DOWN
Q9CY29	<i>Psmc4</i>	26S proteasome non-ATPase regulatory subunit 4	2.62	8.14E-04	1.03E-02	19.12	21.73	UP
A0A1Y7VK19	<i>Isca2</i>	Iron-sulfur cluster assembly 2 homolog, mitochondrial	2.70	8.85E-04	1.10E-02	19.29	21.99	UP
G3UZD6	<i>Ube4b</i>	Ubiquitin conjugation factor E4	1.07	1.16E-03	1.36E-02	19.67	20.75	UP
Q9EQ21	<i>Hamp</i>	Hepcidin	2.13	1.16E-03	1.36E-02	21.69	23.83	UP
B2ZRS3	<i>Deptor</i>	DEP domain-containing mTOR-interacting protein	-1.50	1.28E-03	1.44E-02	23.53	22.03	DOWN
Q8K2H5	<i>Maged1</i>	Melanoma-associated antigen D1	2.09	1.28E-03	1.44E-02	19.67	21.76	UP
Q61408	<i>Gm4788</i>	Gm4788 protein	-2.33	1.35E-03	1.49E-02	21.84	19.50	DOWN
Q3UHE7	<i>Kif21a</i>	Kinesin motor domain-containing protein	1.04	1.36E-03	1.49E-02	23.81	24.84	UP
Q9QYE6	<i>Golga5</i>	Golgin subfamily A member 5	1.56	1.41E-03	1.52E-02	20.73	22.29	UP

Protein ID	Gene Symbol	Protein Name	log2FC (AKI/Sham)	P-value	Adjusted P-value (FDR)	Mean Intensity Sham	Mean Intensity AKI	Regulation
A0A494BBF6	<i>Stub1</i>	E3 ubiquitin-protein ligase CHIP	1.14	1.50E-03	1.59E-02	19.93	21.08	UP
Q544T4	<i>St3gal1</i>	CMP-N-acetylneuraminate-beta-galactosamide-alpha-2,3-sialyltransferase 1	2.53	1.56E-03	1.65E-02	20.24	22.77	UP
A0A0R4J1J3	<i>St3gal5</i>	Lactosylceramide alpha-2,3-sialyltransferase	1.99	1.59E-03	1.67E-02	22.89	24.88	UP
A2BIN1	<i>Mup10</i>	Mup10 protein	-1.66	1.61E-03	1.67E-02	29.64	27.99	DOWN
Q9CR58	<i>Slc25a30</i>	Kidney mitochondrial carrier protein 1	2.38	1.66E-03	1.70E-02	19.56	21.94	UP
Q9CX98	<i>Cyp2u1</i>	Cytochrome P450 2U1	-3.22	1.73E-03	1.74E-02	22.09	18.88	DOWN
Q99JZ7	<i>Errfi1</i>	ERBB receptor feedback inhibitor 1	1.57	1.74E-03	1.74E-02	21.93	23.50	UP
Q8BIL5	<i>Hook1</i>	Protein Hook homolog 1	1.00	1.79E-03	1.77E-02	21.31	22.31	UP
Q9CXK3	<i>Actc1</i>	ACTC protein	-1.12	1.99E-03	1.92E-02	23.64	22.52	DOWN
F8VQ05	<i>Fryl</i>	Fryl protein	2.67	2.06E-03	1.96E-02	19.87	22.55	UP
Q8VCT0	<i>Ldlr</i>	Low-density lipoprotein receptor	-2.47	2.06E-03	1.96E-02	23.05	20.58	DOWN
A8CA96	<i>Tcea3</i>	Transcription elongation factor	-2.23	2.18E-03	2.05E-02	20.86	18.63	DOWN
E9Q1P8	<i>Irf2bp2</i>	Interferon regulatory factor 2-binding protein 2	1.55	2.26E-03	2.10E-02	19.62	21.17	UP
P28651	<i>Ca8</i>	Carbonic anhydrase-related protein	-1.71	2.29E-03	2.12E-02	22.77	21.06	DOWN

Protein ID	Gene Symbol	Protein Name	log2FC (AKI/Sham)	P-value	Adjusted P-value (FDR)	Mean Intensity Sham	Mean Intensity AKI	Regulation
Q99LC9	<i>Pex6</i>	Peroxisomal ATPase PEX6	-1.08	2.50E-03	2.23E-02	23.27	22.20	DOWN
Q9R1Q6	<i>Tmem176b</i>	Transmembrane protein 176B	1.48	2.65E-03	2.30E-02	20.06	21.54	UP
Q9CTW2	<i>Lipe</i>	Hormone-sensitive lipase	-1.48	2.69E-03	2.31E-02	21.01	19.53	DOWN
O08692	<i>Ngp</i>	Neutrophilic granule protein	1.25	2.69E-03	2.31E-02	22.58	23.83	UP
A0A0R4J0T8	<i>Arfgap3</i>	ADP-ribosylation factor GTPase-activating protein 3	2.31	2.72E-03	2.32E-02	19.78	22.09	UP
Q9EQQ9	<i>Mgea5</i>	Protein O-GlcNAcase	1.36	3.05E-03	2.53E-02	19.51	20.87	UP
Q8CC91	<i>Cyp2j6</i>	unspecific monooxygenase	-1.84	3.08E-03	2.54E-02	21.82	19.98	DOWN
Q3TUU3	<i>Acaa1b</i>	Acaa1b protein	-1.22	3.13E-03	2.57E-02	28.67	27.46	DOWN
B7ZMW6	<i>Cd163</i>	Scavenger receptor cysteine-rich type 1 protein M130	2.69	3.35E-03	2.68E-02	20.62	23.31	UP
Q3UGS4	<i>Fam195b</i>	Mapk-regulated corepressor-interacting protein 1	2.18	3.64E-03	2.86E-02	19.22	21.40	UP
A0A097BVN3	<i>Gfra1</i>	GDNF family receptor alpha	1.40	3.73E-03	2.92E-02	21.11	22.51	UP
Q3UN35	<i>B4galnt1</i>	Beta-1,4 N-acetylgalactosaminyltransferase	2.42	3.81E-03	2.97E-02	20.04	22.45	UP
Q547C4	<i>Scd1</i>	stearoyl-CoA 9-desaturase	-1.59	4.05E-03	3.08E-02	25.46	23.87	DOWN

Protein ID	Gene Symbol	Protein Name	log2FC (AKI/Sham)	P-value	Adjusted P-value (FDR)	Mean Intensity Sham	Mean Intensity AKI	Regulation
Q9D1K2	<i>Atp6v1f</i>	V-type proton ATPase subunit F	-2.60	4.08E-03	3.10E-02	21.96	19.37	DOWN
Q8VE91	<i>Fam134b</i>	Reticulophagy regulator 1	2.06	4.12E-03	3.10E-02	19.34	21.40	UP
Q8C094	<i>Mapk9</i>	Stress-activated protein kinase JNK	-2.19	4.28E-03	3.17E-02	23.04	20.85	DOWN
Q80Y55	<i>Bsdcl</i>	BSD domain-containing protein 1	1.14	4.30E-03	3.17E-02	20.62	21.75	UP
Q03311	<i>Bche</i>	Cholinesterase	-1.90	4.44E-03	3.24E-02	23.54	21.65	DOWN
Q4FJZ2	<i>Kpna6</i>	Importin subunit alpha	-1.11	4.74E-03	3.39E-02	23.16	22.05	DOWN
B7ZWM6	<i>Sorbs2</i>	Sorbs2 protein	-2.48	4.84E-03	3.43E-02	21.77	19.30	DOWN
B2RWZ2	<i>Myo1d</i>	Unconventional myosin-Id	2.19	4.93E-03	3.46E-02	19.35	21.54	UP
A0A140T8I9	<i>Pi4ka</i>	Phosphatidylinositol 4-kinase alpha	1.10	5.40E-03	3.69E-02	19.76	20.86	UP
A0A494BBG2	<i>Fam195a</i>	Fam195a protein	-2.47	5.61E-03	3.76E-02	22.05	19.58	DOWN
Q14BE1	<i>Slc35d1</i>	Slc35d1 protein	-1.56	6.27E-03	4.09E-02	25.09	23.52	DOWN
A0A571BEC9	<i>Plin4</i>	Perilipin-4	2.98	6.38E-03	4.14E-02	18.72	21.70	UP
Q8R2Q8	<i>Bst2</i>	Bone marrow stromal antigen 2	-1.76	6.51E-03	4.15E-02	23.05	21.29	DOWN
Q3UVH2	<i>Csk</i>	Tyrosine-protein kinase	-1.02	6.56E-03	4.17E-02	23.49	22.47	DOWN
E9QA15	<i>Cald1</i>	Cald1 protein	3.23	6.83E-03	4.23E-02	18.53	21.77	UP

<b>Protein ID</b>	<b>Gene Symbol</b>	<b>Protein Name</b>	<b>log2FC (AKI/Sham)</b>	<b>P-value</b>	<b>Adjusted P-value (FDR)</b>	<b>Mean Intensity Sham</b>	<b>Mean Intensity AKI</b>	<b>Regulation</b>
Q8VD00	<i>Tmem97</i>	Sigma intracellular receptor 2	-1.74	7.47E-03	4.48E-02	25.02	23.28	DOWN
O35728	<i>Cyp4a14</i>	Cytochrome P450 4A14	3.76	7.62E-03	4.56E-02	20.28	24.04	UP
Q3UPN9	<i>Cebpb</i>	CCAAT/enhancer-binding protein	2.48	7.68E-03	4.58E-02	19.43	21.91	UP
P06728	<i>Apoa4</i>	Apolipoprotein A-IV	1.43	7.84E-03	4.64E-02	21.82	23.25	UP

FC, fold change; FDR, false discovery rate. Significance threshold:  $|\log_2FC| > 0.25$ ,  $FDR < 0.05$

**Table S2. Gene Set Enrichment Analysis (GSEA) of hepatic proteome following AKI**

Pathway Name	Database	Gene Set Size	NES	P-value	FDR q-value	Leading Edge Genes
<b>A. Significantly UPREGULATED pathways (positive NES, FDR &lt; 0.25)</b>						
Network Map Of SARS-CoV-2 Signaling	WikiPathways	73	<b>2.10</b>	3.39e-07	3.90e-05	<i>Lrg1, Fga, Hp, Saa2, Itih4, Ctsl, Fgg, Fgb</i>
Unfolded Protein Response †	Hallmark	48	<b>2.08</b>	1.95e-06	1.27e-05	<i>Fus, Eef2, Arfgap1, Khrrp, Srprb, Eif4a3, Bag3, Dnajc3</i>
Cytoplasmic Ribosomal Proteins	WikiPathways	74	<b>2.05</b>	5.47e-07	3.90e-05	<i>Rpl23a, Rpl18a, Rpl13a, Rps9, Rpl28, Rps27, Rps3a1, Rpl18</i>
Spliceosome	KEGG	82	<b>2.00</b>	5.09e-06	9.51e-05	<i>Ddx5, Fus, Puf60, Snrpf, Eif4a3, Sart1, Rbm8a, Sf3a1</i>
Vitamin B12 Metabolism	WikiPathways	29	<b>1.97</b>	9.91e-05	2.84e-03	<i>Fga, Saa2, Fgg, Fgb, Saa1, Serpina3m, Mat1a, Abca1</i>
Integrin Signaling	KEGG	42	<b>1.93</b>	1.74e-04	2.12e-03	<i>Fga, C3, Fgg, Fgb, Fn1, Vtn, Fermt2</i>
mRNA Processing	WikiPathways	77	<b>1.92</b>	1.57e-05	6.39e-04	<i>Fus, Hnrnp1, Snrpf, Sfpq, Sf3a1, Srsf5, Ppm1g, Sf3b1</i>
IL6 JAK Stat3 Signaling	Hallmark	10	<b>1.85</b>	1.29e-03	4.69e-03	<i>A2m, Stat3, Hmox1</i>
Complement And Coagulation Cascades	KEGG	34	<b>1.84</b>	9.94e-04	1.01e-02	<i>Fga, C3, A2m, Fgg, Kng2, Fgb, Kng1, Clu, Vtn, Serpinf2, Serpina1b</i>
Protein Secretion †	Hallmark	68	<b>1.83</b>	1.56e-04	8.47e-04	<i>Ap3s1, Sec24d, Abca1, Gbfl, Sec22b, Tpd52, Arfgap3, Uso1</i>
Epithelial Mesenchymal Transition †	Hallmark	39	<b>1.78</b>	9.39e-04	4.38e-03	<i>Nnmt, Fn1, Tgm2, Cald1, Lrp1, Fermt2, Calu, Tpm1</i>
Translation Factors	WikiPathways	40	<b>1.77</b>	9.18e-04	1.64e-02	<i>Eif6, Eef2, Pabpc1, Eif3g, Eif4g1, Eif3b, Eif4a1, Eif4h</i>
Blood Clotting Cascade	WikiPathways	10	<b>1.74</b>	4.53e-03	4.61e-02	<i>Fga, Fgg, Fgb, Serpinf2</i>
Folate Metabolism	WikiPathways	35	<b>1.74</b>	2.71e-03	3.87e-02	<i>Fga, Saa2, Fgg, Fgb, Saa1, Serpina3m, Mat1a, Abca1</i>
Neutrophil Extracellular Trap Formation	KEGG	29	<b>1.72</b>	3.93e-03	2.99e-02	<i>Fga, C3, Fgg, Fgb</i>
MirTargeted Genes In Squamous Cell	WikiPathways	61	<b>1.72</b>	1.95e-03	3.27e-02	<i>Fndc3b, Hmox1, Csdel, Atp2a2, Gfpt1, Ptma, Srprb, Akap8</i>
Ribosome	KEGG	138	<b>1.71</b>	6.20e-05	8.38e-04	<i>Mrps5, Rpl23a, Mrps7, Mrps33, Rpl18a, Rpl13a, Rps9, Rpl28</i>
Affected Pathways In Duchenne Muscular Dystrophy	WikiPathways	19	<b>1.71</b>	7.56e-03	6.58e-02	<i>Fga, Fgg, Fgb</i>

Pathway Name	Database	Gene Set Size	NES	P-value	FDR q-value	Leading Edge Genes
Burn Wound Healing	WikiPathways	16	<b>1.65</b>	8.13e-03	6.70e-02	<i>Ambp, Fn1, Tpt1, S100a9</i>
Cytoskeleton In Muscle Cells	KEGG	74	<b>1.64</b>	2.72e-03	2.28e-02	<i>Fn1, Sptbn1, Zyx, Plec, Myh9, Lmna, Sptan1, Tpm1</i>
Complement System	WikiPathways	33	<b>1.63</b>	1.09e-02	8.15e-02	<i>Fga, C3, Fgg, Fgb, Apcs, Vtn</i>
Coagulation	Hallmark	60	<b>1.59</b>	4.65e-03	1.52e-02	<i>Fga, C3, Ctsl, A2m, Fgg, Fn1, Clu, Lrp1</i>
Hypoxia	Hallmark	51	<b>1.57</b>	5.92e-03	1.75e-02	<i>Cp, Tgm2, Pck1, Hmox1, Hdlbp, Mt1, Aldoa, Plin2</i>
Proteoglycans In Cancer	KEGG	58	<b>1.55</b>	1.08e-02	6.94e-02	<i>Ctsl, Fn1, Stat3, Ddx5, Vtn, Ppp1r12a, Ctn, Actb</i>
G2/M Checkpoint	Hallmark	49	<b>1.52</b>	1.42e-02	3.86e-02	<i>Sjfq, Rbm14, Kif5b, Srsf1, Numa1, Chmp1a, Syncrip, Ncl</i>
MirTargeted Genes In Muscle Cell	WikiPathways	133	<b>1.51</b>	3.90e-03	4.61e-02	<i>Fndc3b, Hmox1, Csde1, Atp2a2, Gfpt1, Ptma, Srprb, Lrp1</i>
Coronavirus Disease - COVID-19	KEGG	104	<b>1.46</b>	9.19e-03	6.20e-02	<i>Fga, C3, Fgg, Fgb, Stat3, Rpl23a, Rpl18a, Rpl13a</i>

#### B. Significantly DOWNREGULATED pathways (negative NES, FDR < 0.25)

Pentose And Glucuronate Interconversions	KEGG	23	<b>-2.36</b>	3.45e-09	8.39e-07	<i>Dcxr, Fggy, Ugt1a1, Xylb, Akr1a1, Sord, Ugt1a6b, Dhdh</i>
Disorders Of Bile Acid Synthesis And Biliary Transport †	WikiPathways	21	<b>-2.33</b>	5.97e-08	1.70e-05	<i>Akr1d1, Baat, Slc10a1, Abcb4, Abcb11, Amacr, Hsd3b7, Scp2</i>
Steroid Hormone Biosynthesis †	KEGG	45	<b>-2.28</b>	4.62e-08	3.35e-06	<i>Hsd17b6, Hsd11b1, Srd5a1, Akr1d1, Cyp2c70, Hsd3b5, Cyp3a25, Cyp2d22</i>
Bile Acid Metabolism †	Hallmark	78	<b>-2.28</b>	2.30e-09	7.51e-08	<i>Slc22a18, Slc27a5, Hacd1, Agxt, Sod1, Gmmt, Hsd17b6, Dio1</i>
Serotonergic Synapse	KEGG	33	<b>-2.28</b>	9.82e-08	4.50e-06	<i>Itp2, Mapk3, Cyp2c70, Prkacb, Cyp2d22, Cyp2c54, Cyp2c67, Cyp2c68</i>
Peroxisome †	KEGG	64	<b>-2.26</b>	5.06e-08	3.35e-06	<i>Pex11b, Nudt12, Pex7, Pex26, Acnat1, Dhra4, Pex3, Hacd1</i>
Retinol Metabolism	KEGG	45	<b>-2.25</b>	1.11e-07	4.50e-06	<i>Hsd17b6, Rdh16, Cyp2c70, Adh1, Cyp3a25, Cyp2c54, Cyp2c67, Ugt1a1</i>
Ascorbate And Aldarate Metabolism	KEGG	20	<b>-2.24</b>	5.52e-08	3.35e-06	<i>Rgn, Ugt1a1, Akr1a1, Ugt1a6b, Aldh3a2, Ugt2b35, Ugt2a3, Ugt2b1</i>
Drug Metabolism - Cytochrome P450	KEGG	42	<b>-2.23</b>	2.75e-07	9.56e-06	<i>Ugt1a9, Gsto1, Adh4, Gstm2, Gstm7, Gstm3, Gstm3</i>
Metabolism Of Xenobiotics By Cytochrome P450	KEGG	40	<b>-2.21</b>	6.16e-07	1.87e-05	<i>Ugt1a9, Gsto1, Adh4, Gstm2, Gstm7, Hsd11b1, Gstm3</i>
Oxysterols Derived From Cholesterol	WikiPathways	27	<b>-2.20</b>	3.11e-06	1.48e-04	<i>Hsd11b1, Akr1d1, Baat, Acot8, Amacr, Hsd3b7, Acot12, Scp2</i>

Pathway Name	Database	Gene Set Size	NES	P-value	FDR q-value	Leading Edge Genes
Peroxisome †	Hallmark	63	<b>-2.19</b>	2.63e-07	3.56e-06	<i>Cadm1, Idh1, Acot8, Abcb4, Pex14, Acs15, Ehhadh, Hsd3b7</i>
Chemical Carcinogenesis - DNA Adducts	KEGG	47	<b>-2.17</b>	1.44e-06	3.18e-05	<i>Gstm2, Gstm7, Hsd11b1, Nat2, Gstm3, Mgst1</i>
Drug Metabolism - Other Enzymes	KEGG	55	<b>-2.16</b>	9.16e-07	2.47e-05	<i>Ces1e, Ugt1a9, Gsto1, Tpm1, Nme3, Gstm2, Gstm7</i>
Bile Secretion †	KEGG	37	<b>-2.14</b>	3.27e-06	6.62e-05	<i>Baat, Prkacb, Slc10a1, Abcb4, Abcb11, Ugt1a1, Ugt1a6b, Ldlr</i>
Metapathway Biotransformation Phase I And II	WikiPathways	72	<b>-2.12</b>	4.89e-07	3.90e-05	<i>Mgst1, Gstm7, Akr1d1, Baat, Cyp4v3, Cyp3a25, Cyp2d22, Gsta3</i>
Oxidation By Cytochrome P450	WikiPathways	24	<b>-2.06</b>	6.59e-05	2.35e-03	<i>Cyp4v3, Cyp3a25, Cyp2d22, Cyp4f15, Cyp27a1, Cyb5r3, Cyp2u1, Cyb5a</i>
Arachidonic Acid Metabolism	KEGG	28	<b>-2.06</b>	3.37e-05	5.46e-04	<i>Ptgr2, Cyp2c70, Cyp2c54, Cyp2c67, Cyp2c68, Cyp4a12a, Cyp2c37, Cyp2j6</i>
Glucuronidation	WikiPathways	13	<b>-2.05</b>	9.96e-05	2.84e-03	<i>Ugt1a1, Ugt1a6b, Ugp2, Ugt2b35, Ugt2a3, Ugt2b1, Ugt2b36, Ugt2b34</i>
Biosynthesis Of Cofactors	KEGG	93	<b>-2.04</b>	1.02e-06	2.48e-05	<i>Lipt1, Coasy, Gphn, Pnpa, Rgn, Gclm, Spr, Ugt1a1</i>
Biosynthesis Of Unsaturated Fatty Acids	KEGG	23	<b>-2.04</b>	4.62e-05	7.02e-04	<i>Elovl6, Hacd3, Baat, Elovl2, Acox3, Acaa1a, Scp2, Scd1</i>
ADHD And Autism ASD Pathways	WikiPathways	100	<b>-2.03</b>	7.03e-07	4.01e-05	<i>Sod1, Gmmt, Akt2, Pdxk, Ahcy, Prkacb, Agmo, Gphn</i>
Fatty Acid Metabolism †	KEGG	46	<b>-2.03</b>	3.12e-05	5.42e-04	<i>Acads, Ppt2, Elovl6, Fasn, Hacd3, Acadsb, Acs15, Ehhadh</i>
Tryptophan Metabolism	KEGG	33	<b>-2.02</b>	5.31e-05	7.60e-04	<i>Aldh9a1, Afmid, Dhk1, Maob, Hadha, Dld, Dlst, Aldh7a1</i>
Fatty Acid Metabolism †	Hallmark	115	<b>-2.02</b>	5.35e-07	4.36e-06	<i>Hibch, Fasn, Gcdh, Sucla2, Eci1, Gstm7, Mcee, Adh1</i>
Xenobiotic Metabolism †	Hallmark	128	<b>-2.01</b>	3.27e-07	3.56e-06	<i>Adh1, Idh1, Dhfr1, Apoe, Gsta3, Dcxr, Fah, Cndp2</i>
7-OxoC And 7-BetaHC Pathways	WikiPathways	21	<b>-1.96</b>	4.45e-04	1.02e-02	<i>Slc27a5, Hsd11b1, Baat, Acot8, Amacr, Acot12, Scp2, Cyp27a1</i>
Omega-6 Fatty Acids In Senescence	WikiPathways	21	<b>-1.95</b>	4.64e-04	1.02e-02	<i>Cbr1, Gstm7, Ptgs1, Lta4h, Ptgs2, Gpx1, Ptgr2, Cyp4f15</i>
Codeine And Morphine Metabolism	WikiPathways	11	<b>-1.95</b>	3.30e-04	8.55e-03	<i>Cyp2d22, Ugt1a1, Ugt1a6b, Ugt2b35, Ugt2b1, Ugt2b36, Ugt2b34, Slco1b2</i>
Primary Bile Acid Biosynthesis †	KEGG	14	<b>-1.95</b>	1.08e-04	1.38e-03	<i>Acnat1, Slc27a5, Akr1d1, Baat, Acot8, Amacr, Hsd3b7, Scp2</i>
Omega-3 Fatty Acids In Senescence	WikiPathways	15	<b>-1.92</b>	8.71e-04	1.64e-02	<i>Gstm7, Ptgs1, Cyp3a11, Lta4h, Cyp2d22, Elovl2, Ephx2, Fads1</i>
Disorders Of Folate Metabolism And Transport	WikiPathways	10	<b>-1.92</b>	5.14e-04	1.05e-02	<i>Aldh1l1, Shmt1, Qdpr, Shmt2, Ftcdd, Mthfd1</i>



Pathway Name	Database	Gene Set Size	NES	P-value	FDR q-value	Leading Edge Genes
Cholestasis	WikiPathways	10	<b>-1.71</b>	8.23e-03	6.70e-02	<i>Slc10a1, Abcb4, Abcb11, Ldlr, Slc22a1, Ephx1</i>
Fluoropyrimidine Activity	WikiPathways	13	<b>-1.70</b>	1.08e-02	8.15e-02	<i>Dpyd, Upp2, Ces1d, Dpys, Abcg2, Cyp2a5</i>
NRF2 Pathway	WikiPathways	51	<b>-1.70</b>	2.20e-03	3.48e-02	<i>Slc2a2, Gsta3, Gclm, Ugt1a1, Prdx6, Gclc, Ces1d, Slc2a9</i>
Progesterone-Mediated Oocyte Maturation	KEGG	15	<b>-1.70</b>	9.71e-03	6.38e-02	<i>Akt2, Mapk3, Prkacb, Mapk9, Mapk1, Hsp90aa1, Hsp90ab1</i>
Longevity Regulating Pathway	KEGG	20	<b>-1.68</b>	5.03e-03	3.60e-02	<i>Akt1s1, Prkag1, Prkaa2, Hspa8, Prkab1, Sod1, Akt2, Hspa1b</i>
Fatty Acid Degradation	KEGG	39	<b>-1.67</b>	3.57e-03	2.80e-02	<i>Aldh7a1, Acads, Gcdh, Eci1, Adh1, Acadsb, Acsi5, Ehhadh</i>
Nuclear Receptors Metapathway	WikiPathways	103	<b>-1.64</b>	2.40e-03	3.61e-02	<i>Gstm7, Slco2b1, Fasn, Apoc3, Mgst1, Baat, Slc10a1, Abcb4</i>
Histidine Metabolism	KEGG	14	<b>-1.63</b>	1.20e-02	7.50e-02	<i>Hal, Aldh9a1, Maob, Amdhd1, Aldh7a1, Cndp2, Aldh3a2, Uroc1</i>
Cholesterol Biosynthesis Pathway In Hepatocytes	WikiPathways	65	<b>-1.59</b>	5.32e-03	4.90e-02	<i>Akr1d1, Baat, Acot8, Sc5d, Abcb11, Hsd17b2, Elovl2, Amacr</i>
Carbon Metabolism	KEGG	84	<b>-1.47</b>	1.29e-02	7.82e-02	<i>Me1, Agxt2, Eno1, Sdha, Sdhc, Gldc, Pgk1, Pfkf</i>
Chemical Carcinogenesis - Reactive Oxygen Species	KEGG	119	<b>-1.40</b>	1.40e-02	8.28e-02	<i>Cox5a, Gstm2, Gstt1, Sod1, Gstm7, Uqcrc2, Akt2, mtAtp6</i>

NES, normalized enrichment score; FDR, false discovery rate. Pathways with FDR < 0.25 considered significant. Pathways discussed in main text. Leading edge genes shown are the top contributors to enrichment.

**Table S3. Antibodies used in this study**

Target Protein	Host Species	Clonality	Vendor	Catalog Number	RRID	Dilution (WB)	Dilution (IHC)	Application
GRP78/BiP	Rabbit	Monoclonal	Cell Signaling Technology	#3177	AB_2119845	1:1000	—	WB
CHOP/DDIT3	Mouse	Monoclonal	Cell Signaling Technology	#2895	AB_2089254	1:1000	—	WB
ApoB	Rabbit	Polyclonal	Abcam	ab20737	AB_449929	1:1000	—	WB
TLR4	Rabbit	Monoclonal	Cell Signaling Technology	#14358	AB_2798529	1:1000	—	WB
MyD88	Rabbit	Polyclonal	Cell Signaling Technology	#4283	AB_10547882	1:1000	—	WB
CD68	Rat	Monoclonal	Abcam	ab53444	AB_869007	—	1:200	IHC
F4/80	Rat	Monoclonal	Abcam	ab11110	AB_297810	—	1:200	IHC
$\beta$ -Actin	Mouse	Monoclonal	Cell Signaling Technology	#3700	AB_2242334	1:5000	—	WB
GAPDH	Rabbit	Monoclonal	Cell Signaling Technology	#2118	AB_561053	1:5000	—	WB

WB, Western blot; IHC, immunohistochemistry; RRID, Research Resource Identifier. RRIDs were obtained from the Antibody Registry (antibodyregistry.org).

**Table S4. Primer sequences used for quantitative real-time PCR**

<b>Gene Symbol</b>	<b>Forward Primer (5'→3')</b>	<b>Reverse Primer (5'→3')</b>
<i>Hspa5</i>	ACTTGGGGACCACCTATTCCT	ATCGCCAATCAGACGCTCC
<i>Ddit3</i>	CTGCCTTTCACCTTGGAGAC	CGTTTCCTGGGGATGAGATA
<i>Xbp1s</i>	CTGAGTCCGAATCAGGTGCAG	GTCCATGGGAAGATGTTCTGG
<i>Xbp1t</i>	AAGAACACGCTTGGGAATGG	ACTCCCCTTGGCCTCCAC
<i>Apob</i>	GCCCATTGTGGACAAGTTGATC	CCAGGACTTGGAGGTCTTGGA
<i>Tnf</i>	CCCTCACACTCAGATCATCTTCT	GCTACGACGTGGGCTACAG
<i>Il1b</i>	GCAACTGTTCTGAACCTCAACT	ATCTTTTGGGGTCCGTCAACT
<i>Il6</i>	TAGTCCTTCTACCCCAATTTCC	TTGGTCCTTAGCCACTCCTTC
<i>Mtp</i>	CCAGGAAAGGTTCTCTATGCC	GACTCTCTGATGTCGTTGCTTGC
<i>Cd14</i>	TTGAACCTCCGCAACGTGTCGT	CGCAGGAAAAGTTGAGCGAGTG
<i>Md-2</i>	CTGAACCCTGCATAAGACTGAGG	CTTCCTTACGCTTCGGCAACTC
<i>F4/80</i>	CGTGTTGTTGGTGGCACTGTGA	CCACATCAGTGTTCCAGGAGAC
<i>Cd68</i>	GGCGGTGGAATACAATGTGTCC	AGCAGGTCAAGGTGAACAGCTG
<i>Cd163</i>	GGCTAGACGAAGTCATCTGCAC	CTTCGTTGGTCAGCCTCAGAGA
<i>Fabp1</i>	AGGAGTGCGAACTGGAGACCAT	GTCTCCATTGAGTTCAGTCACGG
<i>Acox1</i>	GCCATTCGATACAGTGCTGTGAG	CCGAGAAAAGTGGAAAGGCATAGG
<i>GAPDH</i>	AGGTCGGTGTGAACGGATTTG	TGTAGACCATGTAGTTGAGGTCA

All primers designed for *Mus musculus* (mouse).